

Texture Characterization of Carotid Atherosclerotic Plaque from B-mode Ultrasound Using Gabor Filters

John Stoitsis, *Member, IEEE*, Spyretta Golemati, *Member, IEEE*, Nikolaos Tsiaparas, and Konstantina S. Nikita, *Senior Member, IEEE*

Abstract— Texture analysis of B-mode ultrasound images of carotid atheromatous plaque can be valuable for the accurate diagnosis of atherosclerosis. In this paper, Gabor filters were used to characterize the texture of carotid artery atherosclerotic tissue. B-mode ultrasound images of 10 symptomatic and 9 asymptomatic plaques were interrogated. A total of 40 texture features were estimated for each plaque. The bootstrap method was used to compare the mean values of the texture features extracted from the two groups. After bootstrapping, the mean value and the standard deviation of the energy estimated using the Gabor filters was found to be significantly different between symptomatic and asymptomatic plaques in the first scale of analysis and for all orientations. In addition, a number of texture features that correspond to larger resolution scales were found to be significantly different between the two types of plaques. It is concluded that Gabor-filter-based texture analysis in combination with a powerful statistical technique, such as bootstrapping, may provide valuable information about the plaque tissue type.

I. INTRODUCTION

IT has been shown that the instability of the carotid atheromatous plaque may be associated not only with the degree of stenosis but also with plaque echogenicity estimated from B-mode ultrasound images [1]. Plaque echogenicity via image texture analysis has been analyzed with a number of techniques. Texture features derived from statistical [2], [3], model-based [4], [3] and Fourier-based [3] methods have been used to characterize and classify carotid atheromatous plaques from B-mode ultrasound.

Gabor functions have been used in a number of vision tasks and they represent many advantages for texture applications [5]. Their advantages include tunable bandwidths, possibility to be defined to operate over a range of spatial frequency channels, and obeying the uncertainty principle in two dimensions [6]. An image can be represented as the sum of output of a bank of filters of 2D Gabor images. The choice of Gabor filtering for texture analysis is based on the evidence from psychophysical research [7] indicating that the human brain performs a

frequency analysis of images. An example of the application of Gabor filters in medical images includes the automatic segmentation and recognition of lungs and lesion from CT scans of thorax [8].

Previous work on texture analysis of atheromatous plaque includes the use of classification and traditional statistical analysis under the assumption that the original sample is sufficiently large to apply ‘asymptotic’ results. The bootstrap technique was introduced as an approach to estimate confidence intervals for parameters in cases for which standard statistical methods cannot be applied [9]. The technique can be used for the estimation of statistical measures without any assumptions about the distribution of the original data. The bootstrap method is extremely valuable in situations where the original data size is small. Recently, the bootstrap technique was used to assist the differential diagnosis of solid breast tumors using small training sets [10].

The purpose of this paper was to investigate the efficiency of Gabor filters to characterize the texture of carotid atherosclerotic plaques from B-mode ultrasound. Furthermore, the use of the bootstrap technique allows validating the texture analysis results.

II. MATERIALS AND METHODS

A. Description of Ultrasound Image Data and Study Design

A total of 19 atheromatous plaques were investigated, of which 10 were symptomatic and 9 asymptomatic. Symptoms included stroke, hemispheric transient ischemic attack and amaurosis fugax. There was no significant difference in the degrees of stenosis between the two groups of plaques (Student’s t-test, p-value=0.93).

For each subject, a sequence of longitudinal images was recorded with an ATL (Advanced Technology Laboratory) Ultramark 4 Duplex scanner and a high resolution 7.5 MHz linear scan head. Scanner settings (dynamic range 60dB, 2D grey map, persistence low, frame rate high) were set at the beginning of the recording and not altered during the procedure. These settings were common for all investigations. Figure 1 shows examples of images from a symptomatic and an asymptomatic subject in which the regions of interest (ROIs), corresponding to plaques, were outlined by an expert. It is pointed out that, although Fig. 1

Manuscript received April 23, 2009.

J. Stoitsis, N. Tsiaparas and K.S. Nikita are with the National Technical University of Athens, 15773 Greece (phone: 30-210-7722285; fax: 30-210-7723557; e-mail: stoitsis@biosim.ntua.gr).

S. Golemati is with the Medical School, National Kapodistrian University of Athens, Greece (e-mail: sgolemati@med.uoa.gr).

shows histogram-equalized images, texture analysis was performed on the original (non-histogram-equalized) image ROIs. In this way, information is extracted from the original image content and not from a post-processed version of it.

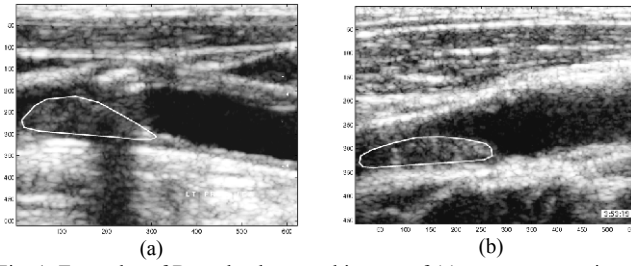


Fig. 1. Examples of B-mode ultrasound images of (a) an asymptomatic and (b) a symptomatic carotid atheromatous plaque. The numbers correspond to the number of pixels from the top and left sides of the image. The plaque boundary was outlined by an expert on the histogram equalized version of the image, because this version enhances visualization of structures of interest.

For each ROI, Gabor-filter-based texture analysis was performed for two different instants of the cardiac cycle, namely systole and diastole. This approach was adopted to ensure that the phase of the cardiac cycle does not affect texture estimation; in addition to this, it allows the investigation of potential texture differences during the cardiac cycle. Gray-scale median (GSM), a widely used feature to characterize carotid atheromatous plaque, was also calculated for each ROI. Statistical evaluation of texture features was performed using bootstrapping.

A. Texture Analysis Using Gabor Filters

Gabor filters are a group of wavelets. A set of filtered images is obtained by convolving the given image with Gabor filters. Each of these images represents the image information at a certain scale and at a certain orientation. From each filtered image, Gabor features can be calculated and used to retrieve images.

For a given image $I(x,y)$ with size $P \times Q$, its discrete Gabor wavelet transform is given by a convolution:

$$G_{mn}(x,y) = \sum_s \sum_t I(x-s,y-t) \cdot \psi_{mn}^*(s,t) \quad (1)$$

where s, t are the filter mask size variables, and ψ_{mn}^* is the complex conjugate of a class of self-similar functions generated from dilation and rotation of the following mother wavelet:

$$\psi(x,y) = \frac{1}{2\pi\sigma_x\sigma_y} e^{-\frac{1}{2}(\frac{x^2}{\sigma_x^2} + \frac{y^2}{\sigma_y^2})} \cdot e^{j2\pi W_x} \quad (2)$$

where W_x is called the modulation frequency. $\psi(x,y)$ is a Gaussian modulated by a complex sinusoid. The self-similar Gabor wavelets are obtained through the generating function:

$$\psi_{mn}(x,y) = a^{-m} \cdot \psi(\tilde{x}, \tilde{y}) \quad (3)$$

where m and n specify the scale and orientation of the wavelet respectively. In addition:

$$\tilde{x} = a^{-m}(x \cos \theta + y \sin \theta) \quad (4)$$

$$\tilde{y} = a^{-m}(-x \sin \theta + y \cos \theta) \quad (5)$$

where $a > 1$ and $\theta = n\pi/N$.

The variables in the above equations are defined as follows:

$$a = \left(\frac{U_h}{U_l}\right)^{\frac{1}{M-1}}, \quad (6)$$

$$W_{m,n} = a^m \cdot U_l \quad (7)$$

$$\sigma_{x,m,n} = \frac{(a+1)\sqrt{2 \ln 2}}{2\pi \cdot a^m (a-1)U_l} \quad (8)$$

$$\sigma_{y,m,n} = \frac{1}{2\pi \tan\left(\frac{\pi}{2N}\right) \sqrt{\frac{U_h^2}{2 \ln 2} - \left(\frac{1}{2\pi\sigma_{x,m,n}}\right)^2}} \quad (9)$$

where a is the scale factor, U_h corresponds to the highest central frequency and U_l to the lowest central frequency of interest.

After applying Gabor filters on the image with different orientation at different scale, we obtain an array of magnitudes:

$$E(m,n) = \sum_x \sum_y |G_{mn}(x,y)| \quad (10)$$

The magnitudes represent the energy at different scale and orientation of the image. Using the transformed coefficients a number of different texture features can be estimated such as the mean μ_{mn} and the standard deviation σ_{mn} :

$$\mu_{mn} = \frac{E(m,n)}{P \cdot Q} \quad (11)$$

$$\sigma_{mn} = \sqrt{\frac{\sum_x \sum_y (|G(x,y)| - \mu_{mn})^2}{P \cdot Q}} \quad (12)$$

where P, Q are the dimensions of the original image.

In order to extract texture features using Gabor filters, the values of parameters corresponding to (i) the lowest and the highest centre frequency (ii) the filter size, (iii) the number of different scales and (iv) the number of different orientations should be properly selected. In this work the selected values for U_l and U_h were 0.05 and 0.4, respectively [11]. The size of the Gabor filter used for texture extraction was 13×13 . To study the texture at different resolution levels the number of different scales was set to 5. In addition, to study the texture directionality in atheromatous

plaque images, four basic orientations were used: horizontal direction (0°), diagonal direction (45°) and (135°), and vertical direction (90°). For each scale and orientation the mean μ_{mn} and standard deviation σ_{mn} of the energy were estimated. Hence, a total of 40 Gabor-based texture features were extracted for each plaque.

B. Statistical Analysis of Texture Features

1) *Feature Selection*: To determine the discriminatory value of each texture feature, a simple statistic figure of merit corresponding to the distance between the two groups was used:

$$dis = \frac{|m_1 - m_2|}{\sqrt{\sigma_1^2 + \sigma_2^2}} \quad (13)$$

where m_1, m_2 are the mean values and σ_1, σ_2 the standard deviations of the two groups. Features that produced dis values greater than a set threshold (in this study 0.57) were retained while the remaining were discarded.

2) *Bootstrap*: The bootstrap method was used to compare the mean values of the texture features extracted from the two investigated groups, i.e., symptomatic and asymptomatic. 10000 bootstrap samples were generated from the original data and the difference of the mean value of samples was used as the statistic to compare the two investigated groups. The statistic was estimated for all the samples and the distribution of the statistic was determined. The proportion of the samples that had a statistic value greater than the actual observed value of the statistic was used to determine the p-value of the bootstrap statistical test.

III. RESULTS

Figure 2 shows examples of images obtained using Gabor filters for the first scale and horizontal direction, for a symptomatic and an asymptomatic plaque. The presence of a horizontal texture pattern in the original image of the symptomatic plaque (Fig. 2, right side) yields increased energy values in the horizontal direction, as can be evidenced by comparing Figs. 2(g) and 2(h).

Tables 1 and 2 show the average values (\pm standard deviations) of texture features for systole and diastole using Gabor filters. Distance values, used for feature selection, as well as bootstrap p-values are also shown in the tables along with GSM values.

Half of texture features that were estimated using Gabor filters for a frame that corresponded to systole, were found to be significantly different between symptomatic and asymptomatic atheromatous plaques. As regards the first scale, both the mean value and the standard deviation were found to be significantly greater for symptomatic plaques. This outcome indicates that differences in the texture of symptomatic and asymptomatic plaques are detected mainly in high frequencies i.e. image details.

In the case of diastole, the mean value and the standard

deviation of the energy were found to be significantly different between symptomatic and asymptomatic plaques in the first scale and for all orientations. In addition, 10 more texture features were found to be significantly different between symptomatic and asymptomatic plaques. The gray level median was not found to be significantly different between the two types of atheromatous plaques.

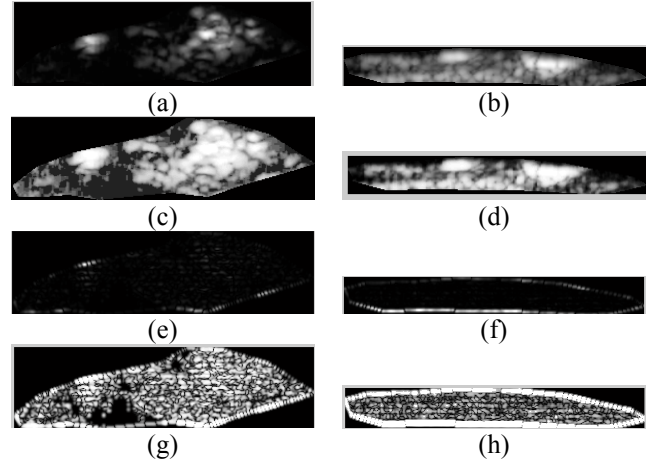


Fig 2: Examples of texture analysis using Gabor filters for an asymptomatic (left column) and a symptomatic (right column) atheromatous plaque for the first scale. (a),(b) original image of asymptomatic plaque, (c),(d) image after histogram equalization (e),(f) horizontal details image (g),(h) horizontal details image after histogram equalization. The images correspond to systole.

TABLE 1: MEAN VALUES (\pm STD) OF TEXTURE FEATURES AND RESULTS OF STATISTICAL ANALYSIS FOR FRAMES THAT CORRESPOND TO SYSTOLE. EMI: ENERGY MEAN FOR SCALE I. ESTDI: ENERGY STANDARD DEVIATION FOR SCALE I.

Texture feature	Symptomatic	Asymptomatic	dis	Bootstrap p-value
EM1 0°	0.443±0.307	0.194±0.073	0.787	0.033
EM1 45°	0.963±0.541	0.451±0.153	0.911	0.015
EM1 90°	2.896±1.242	1.564±0.463	1.005	0.012
EM1 135°	8.178±3.729	4.694±1.417	0.873	0.02
EM2 0°	17.787±11.025	10.485 4.460	0.61	0.077
EM2 45°	0.111±0.040	0.077±0.036	0.626	0.059
EM2 90°	0.380±0.108	0.265±0.116	0.727	0.032
EM2 135°	1.357±0.319	0.965±0.381	0.788	0.027
EM3 90°	0.120±0.034	0.089±0.031	0.655	0.055
EM3 135°	0.280±0.072	0.201±0.064	0.825	0.02
EM4 0°	0.947±0.267	0.679±0.254	0.726	0.034
EM4 45°	3.172±0.908	2.413±0.971	0.571	0.08
EM4 135°	0.105±0.041	0.070±0.025	0.7261	0.036
EM5 0°	0.358±0.108	0.235±0.073	0.937	0.013
EM5 45°	1.277±0.295	0.887±0.281	0.9556	0.01
EM5 90°	3.625±0.784	2.833±0.856	0.682	0.043
ESTD1 0°	1.370±0.714	0.651±0.281	0.9377	0.013
ESTD1 45°	1.851±0.823	0.929±0.342	1.0346	0.0077
ESTD1 90°	4.216±1.445	2.347±0.593	1.1965	0.0024
ESTD1 135°	9.594±2.925	6.296±1.547	0.9964	0.0103
ESTD2 0°	20.37±7.626	14.329±5.414	0.646	0.058
ESTD3 135°	0.458±0.1	0.358±0.124	0.6238	0.0572
ESTD5 0°	0.578±0.163	0.402±0.111	0.8956	0.0134
ESTD5 45°	1.636±0.311	1.281±0.333	0.7794	0.024
Gray level median	31.455±20.191	21.222±12.039	0.43527	0.18

IV. DISCUSSION

In this study, the results of applying Gabor filters to characterize texture of carotid atherosclerotic plaques from B-mode ultrasound were presented. According to the results,

TABLE 2: MEAN VALUES (\pm STD) OF TEXTURE FEATURES AND RESULTS OF STATISTICAL ANALYSIS FOR FRAMES THAT CORRESPOND TO DIASTOLE. EMI: ENERGY MEAN FOR SCALE I. ESTDI: ENERGY STANDARD DEVIATION FOR SCALE I.

Texture feature	Symptomatic	Asymptomatic	dis	Bootstrap p-value
EM1 0°	0.394 \pm 0.194	0.213 0.082	0.861	0.02
EM1 45°	0.9 \pm 0.370	0.503 \pm 0.181	0.964	0.012
EM1 90°	2.802 \pm 0.909	1.785 \pm 0.550	0.957	0.011
EM1 135°	7.625 \pm 3.416	4.968 \pm 1.375	0.722	0.045
EM2 90°	0.390 \pm 0.103	0.288 \pm 0.129	0.621	0.058
EM3 90°	0.118 \pm 0.028	0.090 \pm 0.027	0.701	0.038
EM3 135°	0.293 \pm 0.074	0.217 \pm 0.071	0.736	0.032
EM4 0°	0.981 \pm 0.245	0.765 \pm 0.256	0.609	0.065
EM4 135°	0.103 \pm 0.030	0.076 \pm 0.030	0.636	0.053
EM5 0°	0.359 \pm 0.095	0.269 \pm 0.095	0.668	0.049
EM5 45°	1.306 \pm 0.344	1.002 \pm 0.303	0.664	0.049
ESTD1 0°	1.321 \pm 0.548	0.740 \pm 0.246	0.968	0.013
ESTD1 45°	1.806 \pm 0.614	1.049 \pm 0.312	1.099	0.006
ESTD1 90°	4.137 \pm 1.097	2.685 \pm 0.654	1.137	0.005
ESTD1 135°	9.372 \pm 2.809	6.467 \pm 1.353	0.932	0.013
ESTD2 0°	21.100 \pm 6.205	14.641 \pm 5.228	0.796	0.0244
ESTD3 90°	0.326 \pm 0.082	0.256 \pm 0.090	0.575	0.079
ESTD3 135°	0.477 \pm 0.092	0.375 \pm 0.113	0.7	0.034
Gray level median	29.636 \pm 18.88	21.222 \pm 12.428	0.372	0.246

most of the texture features of symptomatic plaques were found to be statistically different at the 1st and 2nd scale of analysis. This indicates that they differ more in their high rather than in their low spatial frequency patterns. In particular, the images of symptomatic atheromatous plaques preserved a greater amount of energy at the first two scales of analysis compared to that of the images of asymptomatic atheromatous plaques. The higher the value of energy in the 1st scale of analysis, the higher the amount of information which corresponds to fine details of the image. Consequently, in contrast to the asymptomatic atheromatous plaques, the symptomatic seem to concentrate higher energy in the first scales of analysis and therefore to maintain a great amount of fine detail.

Furthermore, the mean value of the GSM of the atheromatous plaques used in this study was not found to be statistically different between symptomatic and asymptomatic plaques [12]. On the contrary, the use of Gabor filters allowed for the estimation of features that are statistically different between the two groups. It is therefore necessary to develop new algorithms based on transformation analysis in order to more accurately characterize the atheromatous plaque.

Moreover, the change in stress of the atheromatous plaques during the cardiac cycle is not expected to cause any statistical difference in texture pattern of ultrasound images. This is expected to be true for symptomatic plaques with high elasticity characterized by lipids and blood. Among the textures of the two different instants of the cardiac cycle, systole and diastole, there was not found any statistical difference, which means that plaques' deformation at different instants of the cardiac cycle does not significantly differentiate the texture pattern.

Finally, it should be pointed out that in order to arrive at safer conclusions the implementation of the suggested approach on a larger sample is considered necessary. The Bootstrap method allows the investigation of the ability of texture features to characterize different types of tissue but can not completely compensate the small sample. It cannot create new data samples from nothing, but it uses samples from the study population. The generated samples are used to study the distribution of statistical measures such as the mean value and standard deviation, as well as the constructing of hypothesis tests.

REFERENCES

- [1] M. L. Grønholdt., B. G. Nordestgaard, T. V. Schroeder, S. Vorstrup, and H. Sillesen, "Ultrasonic echolucent carotid plaques predict future strokes," *Circulation*, vol. 104, no. 1, pp. 68-73, 2001.
- [2] J. E. Wilhjelm, M. L. M. Grønholdt, B. Wiebe, S. K. Jespersen, L. K. Hansen, H. Sillesen, "Quantitative analysis of ultrasound B-mode images of carotid atherosclerotic plaque: correlation with visual classification and histological examination," *IEEE Trans. Med. Imag.*, vol. 17, no. 6, pp. 910-922, Dec. 1998.
- [3] C. I. Christodoulou, C. S. Pattichis, M. Pantziaris, and A. N. Nicolaides, "Texture-based classification of atherosclerotic carotid plaques," *IEEE Trans. Med. Imaging*, vol. 22, no. 7, pp. 902-912, Jul. 2003.
- [4] P. Asvestas, S. Golemati, G. K. Matsopoulos, K. S. Nikita, A. N. Nicolaides, "Fractal dimension estimation of carotid atherosclerotic plaques from B-mode ultrasound: a pilot study," *Ultrasound Med. Biol.*, vol. 28, no. 9, pp. 1129-1136, Sep. 2002.
- [5] D. J. Field, "Relations between the statistics of natural images and the response properties of cortical cells," *J Opt Soc Am A*, vol. 4, no. 12, pp. 2379, 1987.
- [6] M. R. Turner, "Texture segmentation by Gabor functions," *Biol Cybern*, vol. 55, pp. 71-82, 1986.
- [7] B. Julesz, "Nonlinear and cooperative processes in texture perception," in *Theoretical Approaches in Neurobiology*, MIT Press: Cambridge, MA, pp. 93-108, 1981.
- [8] M. Kakar, D. R. Olsen, "Automatic segmentation and recognition of lungs and lesion from CT scans of thorax," *Computerized Med Imaging Graphics*, vol. 33, pp. 72-82, 2009.
- [9] B. Efron, R. J. Tibshirani, *An Introduction to the Bootstrap* New York, Chapman & Hall, 1993.
- [10] D. R. Chen, W. J. Kuo, R. F. Chang, W. K. Moon and C. C. Lee, "Use of the bootstrap technique with small training sets for computer-aided diagnosis in breast ultrasound," *Ultrasound Med. Biol.*, vol. 28, no. 7, pp. 897-902, 2002.
- [11] B.S. Manjunath, W.Y. Ma, "Texture features for browsing and retrieval of image data," *IEEE Transactions on Pattern Analysis and Machine Intelligence (PAMI)*, vol. 18, pp. 837-842, 1996.
- [12] S. Golemati, T.J. Tegos, A. Sassano, K. S. Nikita, A. N. Nicolaides, "Echogenicity of B-mode sonographic images of the carotid artery: work in progress," *J Ultrasound Med.*, vol. 23, no. 5, pp. 659-669, May 2004